

Fuzzy Ternary Particle Systems by Surface-Initiated Atom Transfer Radical Polymerization from Layer-by-Layer Colloidal Core–Shell Macroinitiator Particles

Timothy M. Fulghum, Derek L. Patton, and Rigoberto C. Advincula*

Departments of Chemistry and Chemical Engineering, University of Houston, Houston, Texas 77204

Received January 16, 2006. In Final Form: August 2, 2006

We report the synthesis of ternary polymer particle material systems composed of (a) a spherical colloidal particle core, coated with (b) a polyelectrolyte intermediate shell, and followed by (c) a grafted polymer brush prepared by surface-initiated polymerization as the outer shell. The layer-by-layer (LbL) deposition process was utilized to create a functional intermediate shell of poly(diallyl-dimethylammonium chloride)/poly(acrylic acid) multilayers on the colloid template with the final layer containing an atom transfer radical polymerization (ATRP) macroinitiator polyelectrolyte. The intermediate core–shell architecture was analyzed with FT-IR, electrophoretic mobility (ζ -potential) measurements, atomic force microscopy, and transmission electron microscopy (TEM) techniques. The particles were then utilized as macroinitiators for the surface-initiated ATRP grafting process for poly(methyl methacrylate) polymer brush. The polymer grafting was confirmed with thermo gravimetric analysis, FT-IR, and TEM. The polymer brush formed the outermost shell for a ternary colloidal particle system. By combining the LbL and surface-initiated ATRP methods to produce controllable multidomain core–shell architectures, interesting functional properties should be obtainable based on independent polyelectrolyte and polymer brush behavior.

Introduction

Surface modification through the formation of ultrathin molecular films by the layer-by-layer (LbL) technique has been demonstrated extensively since Decher and co-workers reintroduced the method in the early 1990s.^{1,2} This technique involves the consecutive adsorption of oppositely charged species on a uniformly charged substrate or template. Repeating this simple process gives one the ability to form multilayers with precise control over the total thickness, layer composition, supramolecular structure, and functionality. Films ranging from a few angstroms up to the micrometer level or even higher can be made reliably and reproducibly. The LbL process offers great versatility in deposition of charged species such as polyelectrolytes, nanoparticles, proteins, etc.^{3–5} However, other noncovalent types of interactions have also been utilized. This technique was first adapted to planar substrates, but has more recently been applied to colloidal materials.^{6,7} The preparation of colloidal particles modified by the LbL technique fits into a class of core–shell particle materials in which the outermost shell is comprised of complexed polyelectrolyte layers. Removal of the template core results in the formation of hollow-shell colloidal particle materials.

The core–shell regime has garnered much attention due to its practical application toward controlled delivery and sustained release of drugs⁸ as well as the preparation of hybrid nanomaterials.^{9–11}

An alternative method to modify substrate surfaces includes the grafting of polymer brush architectures.^{12–14} As with the modification of substrates through the LbL method, the interaction of substrates or particles with their surroundings are changed by the addition of polymer brushes or a polymer shell. Surface properties can be easily modified by varying the composition of the polymer brush, grafting density, and the degree of polymerization or MW.^{14–17} There are two distinct pathways to achieve a polymer brush architecture, the first being the “grafting to” approach and the second being the “grafting from” approach. The “grafting to” approach generally utilizes amphiphilic or block polymers with an end functionality that interacts or anchors with the substrate surface. This generally involves a chemical or physical adsorption process. Limitations to this type of application are that the process is diffusion limited so that as more and more polymer chains are attached to the surface, the ability for a new polymer chain to diffuse to the surface of the substrate is greatly hindered.^{12,16} On the other hand, the “grafting from” or surface-initiated polymerization (SIP) approach holds the benefit of placing the initiating groups directly on the surface, allowing

* To whom correspondence should be addressed. E-mail: radvincula@uh.edu.

(1) Decher, G.; Hong, J. D. *Makromol. Chem., Macromol. Symp.* **1991**, *46*, 321.

(2) Decher, G. *Science* **1997**, *277*, 1232.

(3) He, P.; Hu, N.; Rusling, J. F. *Langmuir* **2004**, *20*, 722.

(4) Advincula, R. C.; Park, M. K.; Baba, A.; Kaneko, F. *Langmuir* **2003**, *19*, 654.

(5) Hao, E.; Lian, T. *Langmuir* **2000**, *16*, 7879.

(6) (a) Caruso, F.; Caruso, R. A.; Möhwald, H. *Science* **1998**, *282*, 1111. (b) Radtchenko, I. L.; Sukhorukov, G. B.; Leporatti, S.; Khomutov, G. B.; Donath, E.; Möhwald, H. *J. Colloid Interface Sci.* **2000**, *230*, 272. (c) Sukhorukov, G. B.; Antipov, A. A.; Voigt, A.; Donath, E.; Möhwald, H. *Macromol. Rapid Commun.* **2001**, *22*, 44. (d) Caruso, F.; Donath, E.; Möhwald, H. *J. Phys. Chem. B* **1998**, *102*, 2011. (e) Caruso, F.; Lichtenfeld, H.; Giersig, M.; Möhwald, H. *J. Am. Chem. Soc.* **1998**, *120*, 8523. (f) Donath, E.; Sukhorukov, G. B.; Caruso, F.; Davis, S. A.; Möhwald, H. *Angew. Chem., Int. Ed. Engl.* **1998**, *37*, 2202.

(7) (a) Park, M. K.; Xia, C.; Advincula, R. C.; Schultz, P.; Caruso, F.; *Langmuir* **2001**, *17*, 767. (b) Park, M.-K.; Onishi, K.; Locklin, J.; Caruso, F.; Advincula, R. C. *Langmuir* **2003**, *19*, 8550. (c) Park, M.-K.; Deng, S.; Advincula, R. C. *Langmuir* **2005**, *21*, 5272–5277.

(8) Liu, M. J.; Kono, K.; Frechet, J. M. J. *J. Controlled Release* **2000**, *65*, 121.

(9) Huang, H.; Remsen, E. E.; Kowalewski, T.; Wooley, K. L. *J. Am. Chem. Soc.* **1999**, *121*, 380.

(10) Park, M. K.; Deng, S.; Advincula, R. C. *J. Am. Chem. Soc.* **2004**, *126*, 13723.

(11) Hiller, J.; Rubner, M. F. *Macromolecules* **2003**, *36*, 4078–4083.

(12) Advincula, R.; Brittain, B.; Caster, K.; Ruhe, J., Eds. *Polymer Brushes*; VCH–Wiley: New York, 2004; 483 p.

(13) Kamigaito, M.; Ando, T.; Sawamoto, M. *Chem. Rev.* **2001**, *101*, 3689.

(14) Matyjaszewski, K.; Xia, J. *Chem. Rev.* **2001**, *101*, 2921.

(15) (a) Ejaz, M.; Yamamoto, S.; Ohno, K.; Tsujii, Y.; Fukuda, T.; *Macromolecules* **1998**, *31*, 5934. (b) Ohno, K.; Koh, K.-m.; Tsujii, Y.; Fukuda, T. *Macromolecules* **2002**, *35*, 8989–8993.

(16) Advincula, R.; Zhou, Q.; Park, M.; Wang, S.; Mays, J.; Sakellariou, G.; Pispas, S.; Hadjichristidis, N. *Langmuir* **2002**, *18*, 8672–8684.

(17) Fan, X.; Xia, C.; Fulghum, T.; Park, M.-K.; Locklin, J.; Advincula, R. C. *Langmuir* **2003**, *19*, 916.

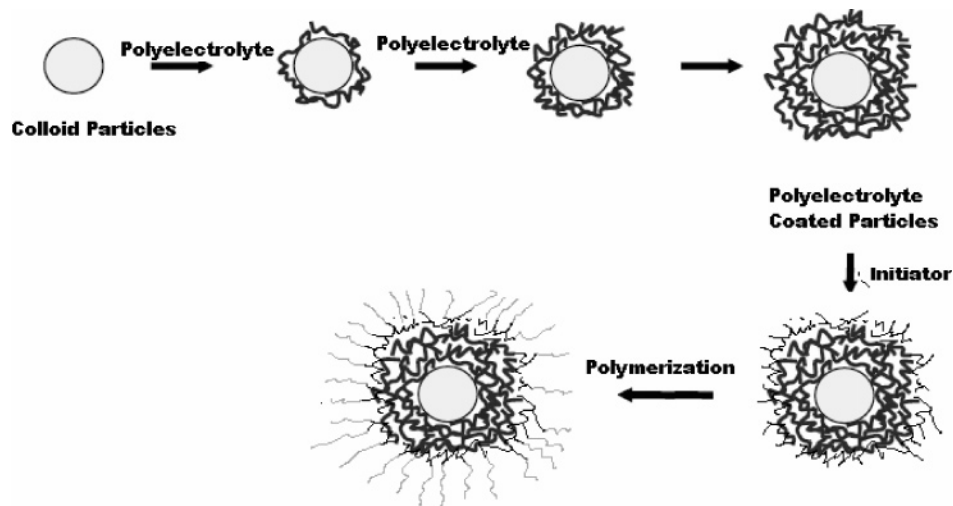


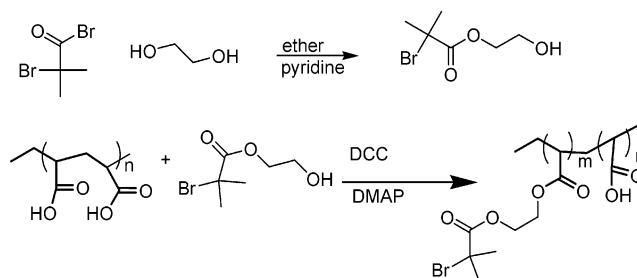
Figure 1. Schematic design of the ternary nanoparticle systems; introduction of a LbL shell of alternating polyelectrolytes with the outermost layer incorporating an ATRP initiator and subsequent polymerization.

synthetic control of the polymer formation.¹³ For example, atom transfer radical polymerization (ATRP) produces near monodisperse polymer chains in the extended “brushlike” architecture.^{14,15} Likewise, living anionic surface-initiated polymerization through surface-bound initiators has also been demonstrated.¹⁶ Recently, a number of publications have appeared showing the feasibility and challenges in grafting polymers from different nanoparticles including gold, carbon black, silica, clays, etc.^{18–21}

In general, coating of particles is carried out to alter the functionality, charge, and/or reactivity of the particle. Stability and dispersibility of the colloidal particles can also be enhanced by the coating process.^{22,23} Core–shell particles formed through the LbL or polymer grafting process have been widely investigated for electro-optical, magnetic, and medicinal applications in recent years.^{24–27} Combining these two coating practices will give a dual layer of control of particle size and morphology, which could be utilized for various technological applications. Selectively choosing materials that form a pH swellable shell, such as poly(allylamine hydrochloride)/poly(acrylic acid), will vary the porosity of the shell;¹⁰ while an outer brush of, e.g., poly(*n*-isopropylacrylamide) will give thermal control over the size and shape of the particle.²⁸

This work involves a feasibility study that combines these two materials synthesis techniques: first, through the formation of core–shell colloidal particles utilizing the LbL method, and second, through the grafting of polymer brushes (Figure 1). The LbL process was first applied by coating with poly(diallyldi-

Scheme 1. Synthesis and Complexation of 2-Hydroxyethyl 2-Bromo-2-methylpropanoate into the Poly(acrylic acid) Backbone To Create a Polyelectrolyte Macroinitiator (Esterified PAA)



methylammonium chloride) (PDADMAC) and poly(acrylic acid) (PAA) on a 400 nm negatively charged sulfate-stabilized polystyrene (PS) core. A polyelectrolyte macroinitiator was then prepared and adsorbed in a few bilayers, leaving the outermost layer of the core–shell architecture with the most exposed initiator groups. Subsequent surface-initiated ATRP polymerization in a bipyridine/CuBr system, with and without free initiator, led to a ternary core–shell particle system with an intermediate polyelectrolyte and outermost polymer brush shell.

Experimental Section

Reagents. PDADMAC (MW < 100 000), PAA (MW < 60 000), bipyridine, CuBr and CuBr₂ salts, dicyclohexylcarbodiimide (DCC), and 4-(dimethylamino)pyridine (DMAP) were used without further purification (from Aldrich Chemical Co.) The negatively charged sulfonated PS particles (400 nm), with a surface area-to-volume ratio of 0.015, were purchased from Microparticles GmbH, Berlin. The water used in all experiments was prepared with a three-stage Millipore Milli-Q Plus purification system and had a resistivity of greater than 18.2 MΩ cm.

Initiator Synthesis. A solution of 2-bromo-2-methyl propionyl bromide (5.7 mL, 46.11 mmol) and diethyl ether (20 mL) was added dropwise, over 1 h, into a mixture of 1,2 ethane diol (3.10 g, 50.0 mmol), pyridine (5.7 mL, 70.5 mmol), and diethyl ether (120 mL) (Scheme 1). This was stirred for a period of 5 h. The reaction mixture was then filtered through a membrane filter collecting the solid byproduct. The 2-hydroxyethyl 2-bromo-2-methylpropanoate product was then washed with water. The ether solution was then concentrated in vacuo producing a colorless oil. The oil was run through a silica column with hexanes as the eluent to purify. ¹H NMR CDCl₃ δ 1.80 (s, 6H); δ 3.62 (t, 2H); δ 3.65 (s, 21); δ 4.21 (t, 2H). The purified material (7.0 g, 31 mmol), PAA (10 g, 135 mmol), and DMAP (100

(18) Raula, J.; Shan, J.; Nuopponen, M.; Niskanen, A.; Jiang, H.; Kauppinen, E. I.; Tenhu, H. *Langmuir* **2003**, *19*, 3499.

(19) Chen, X. Y.; Armes, S. P.; Greaves, S. J.; Watts, J. F. *Langmuir* **2004**, *20*, 587.

(20) Advincula, R. *J. Dispersion Sci. Technol.* **2003**, *24*, 343.

(21) (a) Zhou, Q.; Wang, S.; Fan, X.; Advincula, R.; Mays, J. *Langmuir* **2002**, *18*, 3324–3331. (b) Fan, X.; Xia, C.; Advincula, R. C. *Langmuir* **2005**, *21*, 2537–2544. (c) Fan, X.; Zhou, Q.; Xia, C.; Cristofoli, W.; Mays, J.; Advincula, R. *Langmuir* **2002**, *18*, 4511–4518. (d) Fan, X.; Xia, C.; Advincula, R. C. *Langmuir* **2003**, *19*, 4381–4389.

(22) Liz-Marzan, L. M.; Giersig, M.; Mulvaney, P. *Langmuir* **1996**, *12*, 4329.

(23) Yap, H. P.; Quinn, J. F.; Ng, S. M.; Cho, J.; Caruso, F. *Langmuir* **2005**, *21*, 4328–4333.

(24) Caruso, F.; Spasova, M.; Susha, A.; Giersig, M.; Caruso, R. A. *Chem. Mater.* **2001**, *13*, 109.

(25) Nah, J. W.; Jeong, Y.; Cho, C. S.; Kim, S. *J. Appl. Polym. Sci.* **2000**, *75*, 1115.

(26) Schmidt, H. T.; Gray, B. L.; Wingert, P. A.; Ostafin, A. E. *Chem. Mater.* **2004**, *16*, 4942.

(27) Hu, Y.; Jiang, X.; Ding, Y.; Chen, Q.; Yang, C. *Adv. Mater.* **2004**, *16* (11), 933.

(28) Kim, J. H.; Lee, T. R. *Chem. Mater.* **2004**, *16*, 3647–3651.

mg, 0.8 mmol) were dissolved in dichloromethane (20 mL). DCC (6.386 g, 31 mmol) was dissolved in dichloromethane (10 mL) and added dropwise to the stirring solution at 0 °C, which was then stirred for 20 min. The solution was left to react for another 5 h and allowed to warm to room temperature, after which the solution was filtered to remove urea that had formed during the reaction. The solvent was removed with a rotary evaporator, and the modified PAA polymer precipitated in hexanes. The PAA-alkyl bromide initiator was then dried in a vacuum oven for 24 h at 50 °C, yielding a white powder. A ratio of the integration of the broad methine peak centered at δ 3.6 and the six methyl protons at δ 1.85 gave an inclusion of \sim 30% initiator into the polymer backbone.

Core-Shell Preparation. The LbL technique was used to prepare the core-shell particles following the procedure as described by M \ddot{o} hwald et al.⁶ PDADMAC and PAA solutions were prepared at 1 mg/mL, w/v concentrations. A total of 50 μ L of a 10 wt % PS particle was diluted to 500 μ L with H₂O, and then 500 μ L of the PAA solution was added. An adsorption time of 20 min was used with sonication to ensure complete mixing. Three rinse cycles were performed with centrifugation of the particles at 4400 rpm for 10 min followed by removal of the supernatant and rehydration with 1000 μ L of H₂O. After the final rinse cycle, the particles were hydrated to 500 μ L of solution, and 500 μ L of PDADMAC solution was added, with a 20 min adsorption time. This entire cycle was repeated three times to give a total of four bilayers on the PS particles.

Macroinitiator Deposition. A 1 mg/mL solution of the esterified PAA initiator was prepared for solution deposition at pH 7.0. After the deposition of four PDADMAC/PAA bilayers, the outermost layer was left at PAA, leaving a negative surface charge. The particles were concentrated by centrifugation and rehydrated to 500 μ L. To the particle solution was added 500 μ L of the PDADMAC solution. The same 20 min adsorption time was observed, and the three rinse cycles were repeated as described previously. After concentration, the particles were then treated with the modified PAA solution for the adsorption and washing steps. This was repeated two times to give a total of six bilayers, with the outermost layer being the PAA initiator.

Polymerization of PMMA. A total of 50 mg of the dried initiator modified core-shell particles were added to a Schlenk flask with 54 mg (1.5×10^{-4} mol) of dHBpy, 25 mg of Cu(I)Br, and 5 mg of Cu(II)Br₂. A total of 5 mL of methylmethacrylate (MMA) monomer was added to a second Schlenk flask. Both flasks were flushed with nitrogen gas for 30 min. The MMA was degassed by bubbling nitrogen through the MMA during the purging process. After the 30 min of degassing, a double-tipped needle was connected between the two flasks. The monomer was transferred to the flask containing the CuBr:bpv particle initiator mixture. The flask was then placed in a sonicator to ensure dissolution of the initiator particles. The flask was subsequently subjected to two freeze-pump-thaw cycles to remove any final traces of oxygen. The Schlenk flask was then placed in an oil bath at 60–70 °C for 12–48 h. Upon completion of the polymerization process, the reaction was terminated by continued stirring with exposure to air. The solution was then dissolved in tetrahydrofuran (THF), and then the brush-coated particles were precipitated in methanol. Several reprecipitations were carried out to remove excess monomer.

Polymerization in the presence of 10 μ L of 2-hydroxyethyl 2-bromo-2-methylpropanoate (free initiator) was carried out in the same manner as without free initiator. SEC analysis was then carried out on free PMMA polymer separated from the ternary particles by centrifugation after polymerization in the presence of free initiator: 50 mg of dried initiator modified core-shell particles were added to a Schlenk flask, as well as 10 μ L of 2-hydroxyethyl 2-bromo-2-methylpropanoate with 54 mg (1.5×10^{-4} mol) of dHBpy, 25 mg of Cu(I)Br, and 5 mg of Cu(II)Br₂. A total of 5 mL of MMA monomer was added to a second Schlenk flask. Both flasks were flushed with nitrogen gas for 30 min. After 30 min of degassing the MMA was transferred to the flask containing the initiator with a double-tipped needle. The flask was then sonicated for 10 min to ensure dissolution of the initiator particles, and the flask was subsequently subjected to two freeze-pump-thaw cycles to remove any final traces of

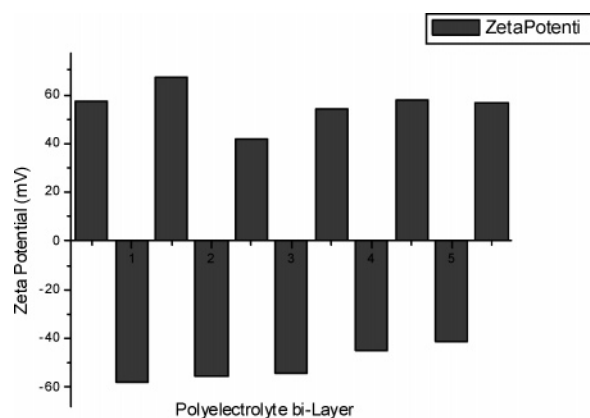


Figure 2. ζ -Potential as a function of polyelectrolyte layer number for (PDADMAC/PAA)-coated 400 nm PS spheres at neutral pH. The even layers correspond to the PDADMAC adsorption and the odd layers to the PAA adsorption.

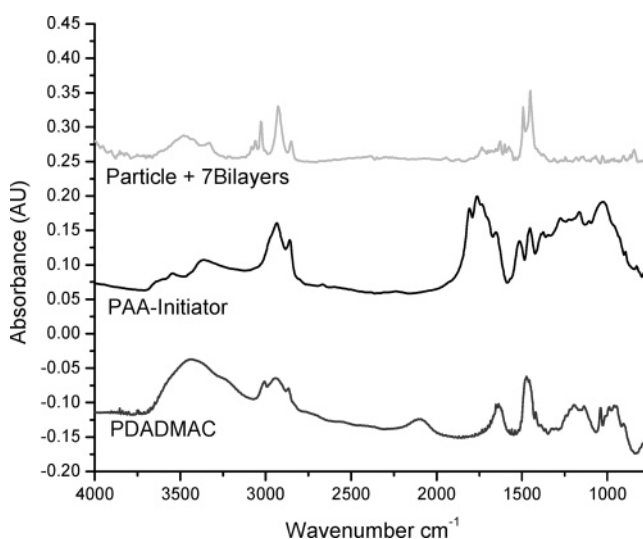


Figure 3. Comparative IR spectra of core shell particle and polyelectrolyte materials used in the LbL process. The PDADMAC spectra (bottom) shows a methyl umbrella peak at 1465 cm^{-1} , the esterified PAA spectra (middle) has a broad C=O stretch in the 1700 cm^{-1} region, and the colloidal particle after layer 12 spectra (top) shows the integration of the methyl umbrella and the carbonyl of the esterified PAA.

oxygen. The Schlenk flask was then placed in an oil bath at 60–70 °C for 12–48 h. After polymerization, the reaction was quenched by stirring in ambient conditions. The reaction mixture was diluted with THF and centrifuged to separate the ternary particles from the free polymer. The supernatant was precipitated and washed with methanol. The polymer was then redissolved in THF and centrifuged again to remove any trace of ternary particles. After the product was purified (the process was repeated twice more to remove all traces of monomer and ternary particles), the sample was then dried in a vacuum oven for 24 h at 60 °C and saved for further analysis. SEC analysis was then performed.

Characterization. FT-IR ATR and transmission spectra were obtained on a Digilab FTS 7000 equipped with a HgCdTe detector from 4000 to 600 (cm^{-1}) wavenumbers. All spectra were taken with a nominal spectral resolution of 4 cm^{-1} in transmission mode. KBr pellets were prepared from particles or polyelectrolytes dried in a vacuum oven for 24 h at 40 °C prior to analysis to remove any residual water. ζ -Potential analysis was carried out with a Brookhaven Zeta PALS dynamic light scattering equipment with BI-9000AT digital autocorrelator at 656 nm wavelength at 23 °C and neutral pH. Transmission electron microscopy (TEM) was performed on a JEOL 2000 FX microscope operating at 200 kV. Films for TEM were prepared by drop-casting dilute solutions of the particles onto

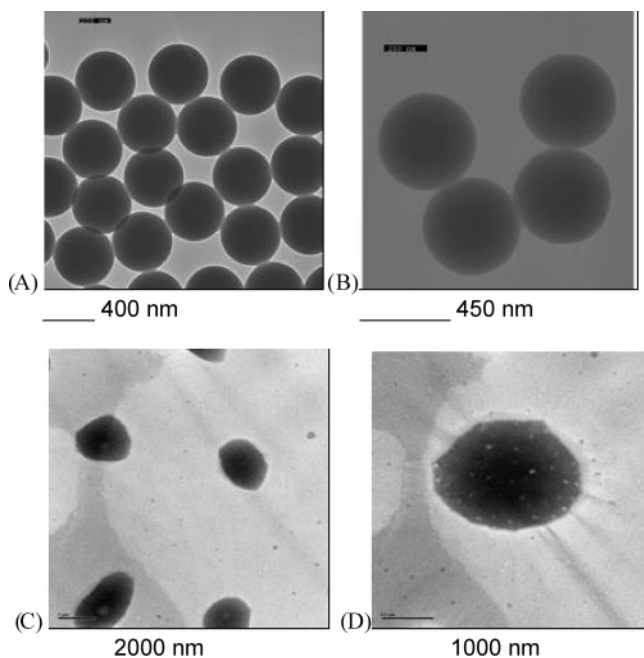


Figure 4. TEM micrographs of (A) the pristine 400 nm PS particles, (B) the particles with a six-bilayer shell of ~ 450 nm showing a slightly roughened surface, and (C, D) particles post-polymerization with a dramatic change in shape and morphology and a size increase to a diameter of ~ 1100 – 1500 nm.

Formvar-coated copper grids. Thermogravimetric analysis (TGA) measurements were made on a TA Instruments model 2050 using N_2 purge gas and a platinum pan. SEC analysis was performed at room temperature using a Viscotek 270 quad detector equipped with VE3210 UV/vis detector and VE3580 RI detector. THF was used as the eluting solvent.

Results and Discussion

The LbL assembly of the PDADMAC/PAA multilayer shell was carried out successfully using the previously described procedure.⁷ The polyelectrolyte deposition process was first analyzed with electrophoretic measurement methods. Figure 2 shows the ζ -potential measurements versus the layer growth of the PDADMAC/PAA polyelectrolyte films on the negatively charged PS core particles. The standard deviation in the measurements ranged from 0.6 to 3.20 mV. The bare PS particle had a ζ -potential of about -65 mV (layer number 0) as shown in Figure 2. The subsequent deposition of PDADMAC and PAA gave alternating surface charges as observed in the ζ -potential measurements up to the 8th layer. The variations in the ζ -potential are of the order of ± 40 – 45 mV range, with the last layer indicating a negative surface charge on the colloidal particle due to the anionic nature of the PAA molecule. This alternating surface charge is indicative of the stepwise growth of the polyelectrolyte multilayer shell. The ζ -potential values observed are typical as reported previously by our group⁷ and by many other groups.^{6,10} In this case, the last two bilayers were composed of PDADMAC/esterified PAA to give bromoisobutyryl ATRP initiator groups on the surface of the particles. Thus, the outermost layer of esterified PAA has a ζ -potential of -45 mV, indicating that the surface charge of the particle is negative, due to the charge on the esterified PAA initiator macromolecule. The PAA is only 30% functionalized with the bromoisobutyryl group which gives it enough negative charge for selective adsorption on the last adsorbed PDADMAC layer.

The growth of the polyelectrolyte shell was also monitored with FT-IR transmission spectroscopy methods. Figure 3 shows

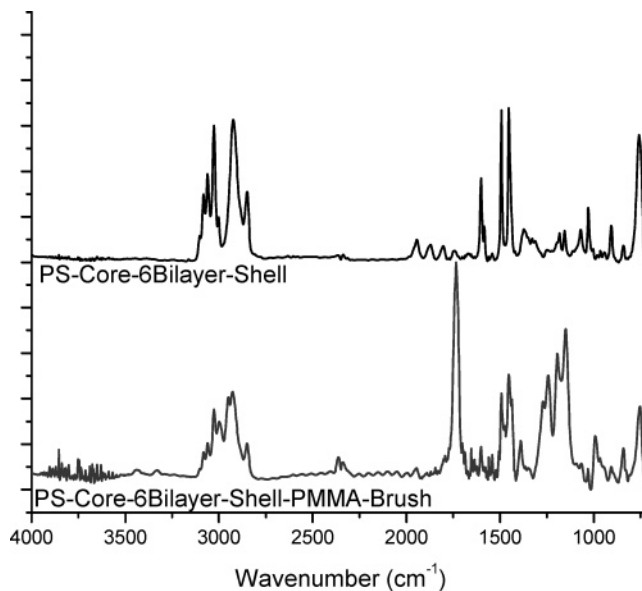


Figure 5. FT-IR spectra of macroinitiator-coated particle, PS-Core-6Bilayer-Shell, and the colloids post PMMA polymerization, PS-Core-6Bilayer-Shell-PMMA-Brush. The ratio of the carbonyl peak at 1740 cm^{-1} to that of the methylene stretching region at 3000 cm^{-1} which represents the PS colloids has greatly increased with post-polymerization.

a composite particle along with the traces from the esterified PAA and PDADMAC. The PDADMAC component can be distinguished by the methyl “umbrella” symmetric bend of the CH groups at 1465 cm^{-1} .²⁵ The esterified PAA component is visible from the presence of the carbonyl stretch at 1740 cm^{-1} . The presence of these peaks is indicative of the successful alternate/composite LbL shell deposition on the colloidal particles.

To view the changes in the colloidal particle morphology with LbL shell deposition, TEM was performed. As shown in Figure 4A, the original particle shows a very smooth and regular surface with a diameter of ~ 400 nm (surface area-to-volume ratio of 0.015). After the formation of the shell through the LbL process, the surface becomes rough and slightly irregular in nature and the diameter also increases to ~ 450 nm, with the surface area-to-volume ratio reduced to 0.013 (Figure 4B).³² For a five-bilayer system, the diameter increases 50 nm, which corresponds to an average layer thickness of approximately ~ 5 nm/polyelectrolyte taking into account that a few base layers are needed before linear growth is seen.^{7,32} This thickness is deemed to be slightly higher than most conventional polyelectrolytes on flat thin films but has been observed in other LbL depositions as well.⁶ This thickness is expected to change with pH as in the case of the presence of a weak polyelectrolyte such as PAA.^{7c}

With the presence of the ATRP initiator on the outer surface, we then proceeded with the ATRP polymerization of poly(methyl methacrylate) (PMMA). PMMA has been previously polymerized by ATRP on a variety of colloidal particles and flat surfaces.¹⁵ A variety of these systems have been reported by a number of groups and is well-defined and studied especially with PMMA.¹⁴ However, we believe that this work is the first instance in which PMMA was grafted from colloidal particles coated with an LbL

(29) Zhao, H.; Argoti, S. D.; Farrell, B. P.; Shipp, D. A. *J. Polym. Sci., Part A: Polym. Chem.* **2004**, *42* (4), 916–924.

(30) Kim, S.; Yoon, S.; Kim, I.; Kim, S. *J. Appl. Polym. Sci.* **2003**, *91* (5), 2876.

(31) Aymonier, C.; Bortzmeyer, D.; Thomann, R.; Mulhaupt, R. *Chem. Mater.* **2003**, *15* (25), 4874.

(32) (a) Lvov, Y.; Decher, G.; Möhwald, H. *Langmuir* **1993**, *9*, 481. (b) Decher, G.; Lvov, Y.; Schmitt, J. *Thin Solid Films* **1994**, *244*, 772.

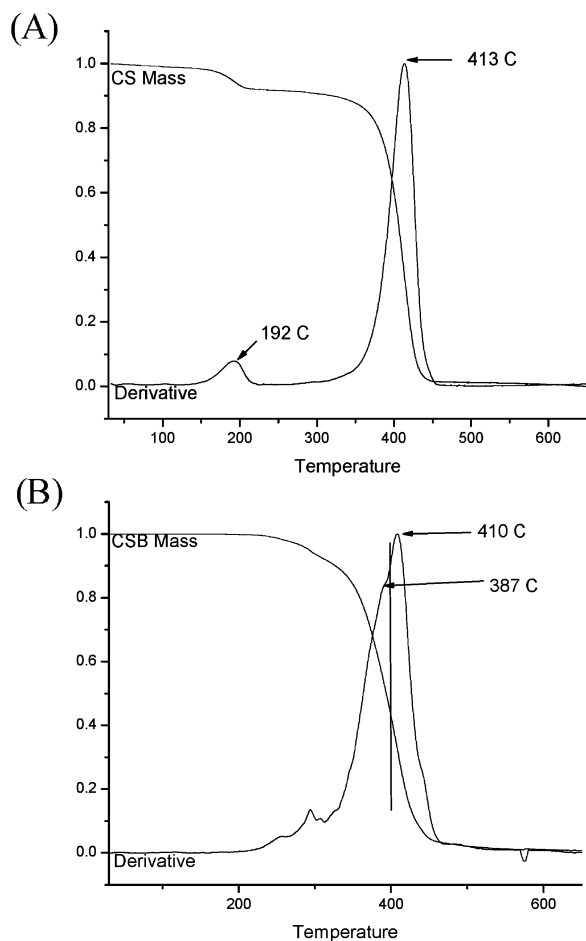


Figure 6. (A) A clear step can be seen with an inflection at 192 °C representing a 7% mass in the particles after 12 layers by the LbL process and another inflection due to the PS core at 413 °C. (B) After a PMMA brush has been grafted from the particles there is a broadening of the lower temperature transition and the introduction of a transition that gives a lower temperature shoulder to the PS transition; this peak max is centered at 387 °C and is attributed to the PMMA brush.

shell where the macroinitiator comprises the last layer of the adsorbed polyelectrolytes. We have previously reported the direct free-radical polymerization of PS on clay nanoparticles adsorbed onto flat solid-support substrates using the LbL method.¹⁷

The core-shell particles above were added to a Schlenk flask in the presence of bipyridine, Cu(I) and Cu(II) ions, with MMA monomer. The reaction was maintained at 60–70 °C for 12–48 h. Upon completion of the polymerization process, the reaction was terminated by continued stirring with exposure to air. After this procedure, the solution was then dissolved in THF and then the brush-coated particles were precipitated in methanol. In this case, the polymerization of PMMA was best analyzed primarily through FT-IR analysis. Figure 5 shows a strong peak at 1740 cm^{-1} showing a dramatic increase in carbonyl stretch due to the ester linkage in the PMMA brush as well as the inclusion of the PS aromatic C=C stretch at 1500 cm^{-1} and the methylene stretch at 3000 cm^{-1} .

TGA was performed to determine degradation properties and the amount of grafted PMMA or percent composition of the PMMA brush with respect to the colloidal core-shell template. As seen in Figure 6A, there are two regions of decomposition in the TGA trace, more easily represented by the derivative curve. The first degradation shows an inflection point centered at 192 °C, and the corresponding mass loss accounts for 6–7% of the total mass of the particles. After polymerization it is difficult to

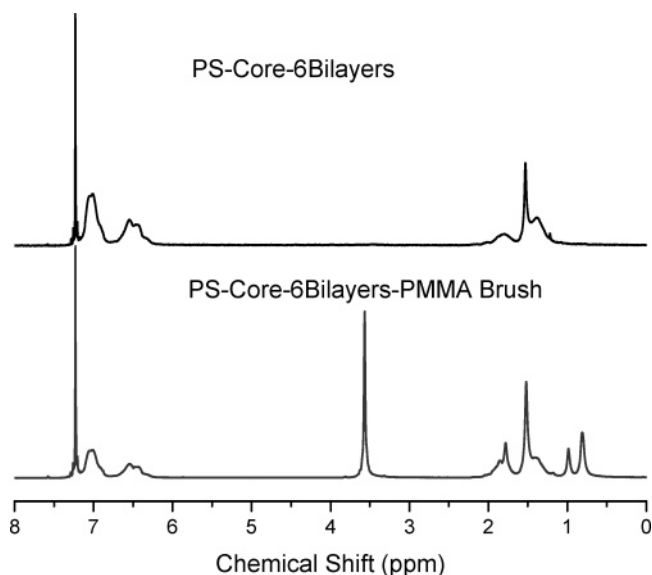


Figure 7. NMR spectra of PS-Core-6Bilayers showing the aromatic protons of the PS core. PS-Core-6Bilayers-PMMA Brush shows the spectra after polymerization and includes the methoxy singlet and the methyl signal at 3.5 and 0.9 ppm, respectively.

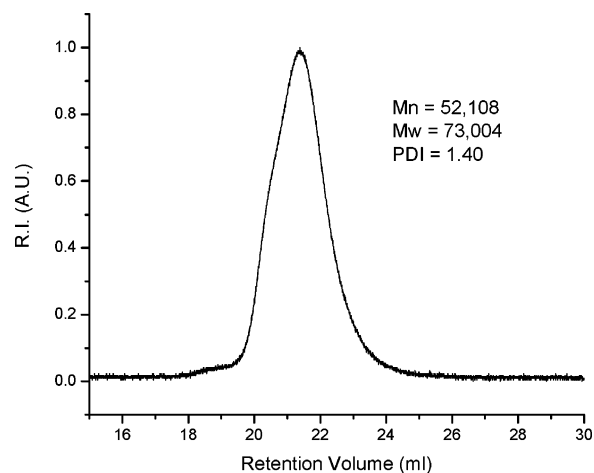


Figure 8. SEC trace of free PMMA from polymerization in the presence of free initiator.

specifically assign the LbL material decomposition; there is still a lower temperature decomposition but it has broadened (Figure 6B) There are two peaks in the derivative curve: one centered at 410 °C for the polystyrene core, and one slightly lower at 387 °C attributed to the PMMA brush. These decomposition temperatures correspond to previous results reported by other groups.^{31,33}

To track the inclusion of PMMA into the structure of the ternary particles, ¹H NMR was performed on both the core-shell particles, as well as the particles post-polymerization (Figure 7). Samples were prepared by dissolution of 10 mg of particles in deuterated chloroform (CDCl_3). In the core-shell spectra the aromatic protons of the PS core can be assigned to the broad multiplets centered at 6.5 and 7 ppm. The broad signal from 1 to 2 is difficult to deconvolute due to the backbone of all three polymers being in the same region. After polymerization, the signal from PMMA is clearly visible from the methoxy singlet at 3.5 ppm and the methyl signal centered at 0.9 ppm which was not originally present. This confirmed structurally the presence of PMMA on the particles.

TEM was used to directly observe the grafting of PMMA from the particles as well (Figure 4C). The particle shape changed drastically from the pristine PS colloidal particle as well as that of the core-shell particle. In both of the previous cases, the particles were still spherical in nature with only a small change in surface morphology. But with post ATRP polymerization, the shape is now oblongated (ellipsoidal) and irregular. In addition, the surface morphology is observed to be rougher. A close-up inspection of Figure 4D possibly reveals the core template with a darker contrast and with the grafted PMMA forming a halo around the particle. But the exact extent of PMMA contribution versus the core-shell is not easily distinguishable by TEM without the use of any contrast agent with the core or the brush shell. Nevertheless, the change in size from ~ 450 to 1100 nm in diameter is quite high, resulting in a decrease in the surface area-to-volume ratio of 0.013 to 0.005 . It is well-known that a large increase in thickness by SIP is a consequence of a lack of MW control due to a very high concentration of monomer compared to initiator.³⁴ This was previously reported for ATRP on particles with sizes greater than 300 nm.³⁴ The change in shape and size is indicative of the successful grafting of the PMMA brush on the surface of the colloid template. However, the exact MW of the grafted polymer is unknown, due to difficulty of implementing a reverse analysis, i.e., degrafting procedure for the tethered polymer brush followed by SEC.

To obtain an approximation of possible macromolecular dimensions of the attached polymer, the second procedure was utilized involving a sacrificial free initiator. The use of a free-initiator together with surface-initiated ATRP has been previously shown to be advantageous for PMMA brushes compared to PS brushes for MW control.³⁴ They serve to lower the initial monomer-to-initiator ratio and to increase the overall initiator concentration, thereby allowing some radical coupling in solution to build up the concentration of deactivator. SEC analysis was carried out on the formed free PMMA polymer separated from the ternary particles by centrifugation after polymerization in the presence of free initiator (second procedure). Thus, after polymerization, the reaction was quenched by stirring in ambient conditions. The reaction mixture was diluted with THF and centrifuged to separate the ternary particles from the free polymer. The supernatant was precipitated and washed with methanol. The polymer was then redissolved in THF and centrifuged again to remove any trace of ternary particles. After the product was purified, SEC was performed (Figure 8.) The sample showed a

polydispersity, $M_w/M_n = 1.4$ with a MW of $73\,000$ g/mol compared to a typical solution ATRP procedure. This MW could not correspond to the large increase in the size of the particle as in the case of the polymerization without the free initiator (first procedure). However, no TEM measurements were done in this sample to correlate this trend. In a controlled SIP-ATRP, this may very well give an approximation of the grafted chain MW and the degree of conversion. Polymerization on particles > 300 nm diameter are known to be model systems for grafting polymer brushes from flat surfaces.³⁴

Future work will involve the synthesis of cleavable macro-initiators and degrafting of the polymers to allow for extensive analysis of the kinetics of polymerization and the macromolecular properties of the grafted polymers. Also, experiments involving pH swelling will be performed to investigate the unique properties of the LbL shell in the presence of an outer shell of grafted PMMA.

Conclusion

This work has demonstrated the concept of combining the two very versatile particle coating methods of layer-by-layer polyelectrolyte adsorption and surface-initiated polymerization in a ternary colloidal polymer particle system. Utilization of a polyelectrolyte macroinitiator and the LbL technique allows the growth of polymer brushes from almost any charged surface. A straightforward synthesis of a polyelectrolyte macroinitiator has been proposed that allows for both the LbL process as well as subsequent ATRP SIP. TEM micrographs were utilized to show the morphological changes that occur during the LbL process as well as after surface polymerization. Thermogravimetric analysis allowed determination of the composition of the polymeric brush component of the ternary structure. Last, the use of a sacrificial free initiator was compared to one without the initiator, and the MW was determined for the free polymer. This ternary material system should be useful in the future for designing new polymer particles with multifunctionality based on the LbL as well as polymer brush shell components.

Acknowledgment. The authors thank Professor Michael Wong and Vinit Murthy of Rice University for help with the ζ -potential measurements and Varian for technical help with FT-IR analysis. The authors also acknowledge funding for the project through Grants DMR-0315565 and CHE-0304807 and the Robert Welch Foundation.

(34) von Werne, T.; Patten, T. *J. Am. Chem. Soc.* **2001**, *123*, 7497.